Research Paper

Optimization of Tensile-Shear Strength in the Dissimilar Joint of Zn-Coated Steel and Low Carbon Steel

Sukarman[1]✉, Amri Abdulah[1], Jatira[1], Dede Ardi Rajab[1], Rohman[1], Choirul Anwar[1], Yulfian Aminanda[2], Muhammad Ali Akbar[3]

[1]Mechanical Engineering Department, Sekolah Tinggi Teknologi Wastukancana, Purwakarta 41151, Indonesia
[2]Mechanical Engineering Department, Universiti Teknologi Brunei, Mukim Gadong A, BE1410, Brunei
[3]Industrial Engineering Department, Sekolah Tinggi Teknologi Wastukancana, Purwakarta 41151, Indonesia

✉ sukarman@stt-wastukancana.ac.id

Check for updates

Abstract

The present study features analytical and experimental results of optimizing resistance spot welding performed using a pneumatic force system (PFS). The optimization was performed to join SECC-AF (JIS G 3313) galvanized steel material with SPCC-SD low carbon steel. The SECC-AF is an SPCC-SD (JIS G 3141) sheet plate coated with zinc (Zn) with a thickness of about 2.5 microns. The zinc coating on the metal surface causes its weldability to decrease. This study aims to obtain the highest tensile-shear strength test results from the combination of the specified resistance spot welding parameters. The research method used the Taguchi method using four variables and a combination of experimental levels. The experimental levels are 2-levels for the first parameter and 3-levels for other parameters. The Taguchi optimization experimental results achieved the highest tensile-shear strength at 5821.10 N. It properly worked at 22 squeeze time cycles, 27 kA of welding current, and 0.5-second welding time and 12 holding-time cycles. The S/N ratio analysis found that the welding current had the most significant effect, followed by welding time, squeeze time, and holding time. The delta S/N ratio values were 1.05, 0.67, 0.57 and 0.29, respectively.

Keywords: Resistance spot welding; Taguchi method; Galvanized steel; S/N ratio; Tensile shear strength

Abstrak

Studi ini menampilkan hasil analitis dan eksperimental pengoptimalan pengelasan titik resistansi yang dilakukan menggunakan sistem gaya pneumatik (PFS). Optimasi dilakukan untuk menggabungkan material baja galvanis SECC-AF (JIS G 3313) dengan baja karbon rendah SPCC-SD. SECC-AF adalah pelat lembaran SPCC-SD (JIS G 3141) yang dilapisi seng (Zn) dengan ketebalan sekitar 2,5 mikron. Lapisan seng pada permukaan logam menyebabkan daya lasnya menurun. Penelitian ini bertujuan untuk mendapatkan hasil uji kuat geser-geser tertinggi dari kombinasi parameter pengelasan titik tahanan yang ditentukan. Metode penelitian menggunakan metode Taguchi dengan menggunakan empat variabel dan kombinasi level eksperimen. Tingkat eksperimental terdiri dari 2 tingkat untuk parameter pertama dan 3 tingkat untuk parameter lainnya. Hasil eksperimen optimasi Taguchi mencapai kekuatan geser-tarik tertinggi pada 5821,10 N. Ini bekerja dengan baik pada 22 siklus waktu pemerasan, arus pengelasan 27 kA, dan waktu pengelasan 0,5 detik, dan 12 siklus waktu penahanan. Analisis S/N ratio menunjukkan bahwa arus pengelasan berpengaruh paling nyata, diikuti waktu pengelasan, waktu pemerasan, dan waktu penahanan. Nilai rasio delta S/N masing-masing adalah 1,05, 0,67, 0,57 dan 0,29.

Kata-kata kunci: *Pengelasan tempat resistensi; Metode Taguchi; Baja galvanis;* S/N ratio; *Kekuatan geser tarik*

1. Introduction

Galvanized steel is steel coated with liquid zinc (Zn) so that it has good corrosion resistance [1]. Data from the Ministry of Industry of the Republic of Indonesia have shown that the demand for galvanized steel for the national automotive industry reaches one million tons per year, and 80% was used for national automobile production [2]. Since 2018, the Indian government has requested that automaker use 70 percent galvanized steel in car body [3]. The increasing growth of the automotive industry demands the need for efficiency and effectiveness of the manufacturing process, and resistance spot welding (RSW) metal alloying techniques are one of the solution. The RSW joining technique has several advantages: more substantial connection results, not requiring fillers, easy application (It does not require special skills), cheap process, and efficient process [4]. RSW is the most popular joining method for steel body structures. Most of the connection methods on automotive bodies also use the RSW joining method [5]–[8]. In particular, their use in the automotive industry is of great importance, as each automobile includes about 5,000 point welds in the assembly process [9].

There are several of metal joining techniques that commonly used in the manufacturing industry, such as Gas Metal Arc Welding (GMAW), Flux Cored Arc Welding (FCAW), and others [10]. GMAW and RSW welding techniques are commonly used in the automotive industry, bridge and building construction, office equipment industry, and households [11]. **Figure 1** shows the difference in the results of the RSW and GMAW / GTAW welding techniques [12].
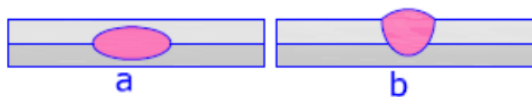

Figure 1. Comparison between RSW (a) and GMAW/GTAW (b)

Resistance spot welding (RSW) is a metal welding technique that provides by an electrical resistance as a heat source on two or more metal surfaces, which causes fusion to form in the welding area [10], [13] Metal melting occurs in welding contacts due to heat generated from contact resistance from electric currents. Electrical

resistance also occurs at the contact between the electrode and the plate. However, metal melting does not occur because both ends of the electrode cooled with the water [14]. The fusion process occurs on the metal surface, which sticks together to melt due to electrical resistance. The RSW process occurs during particular cycle time. The welding current, welding time, and electrode force are the essential process parameters [15]. The RSW scheme is shown in **Figure 2** [11], [16].
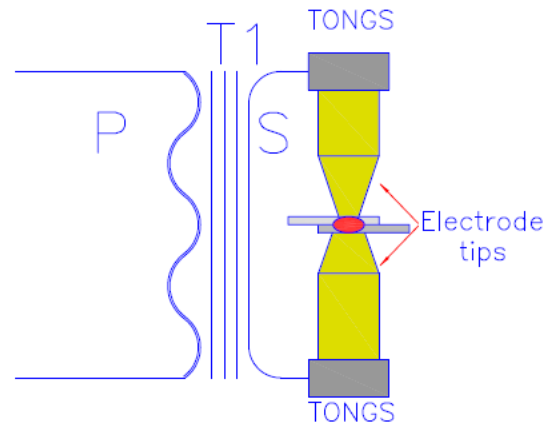

Figure 2. Schematic of resistance spot welding

The joining process of metal works by applying pressure with a pair of electrodes on the metal surface, where the emphasis is applied throughout the RSW cycle [16], [17]. The process of pressuring the RSW starts at the squeeze time cycle. The pressing process serves to prevent deformation (bending) of joints and forge of the metal at the welding area after heating. The welding process occurs when the current flow to the end of the electrode so that the two metal surfaces become melted and fusion occurs between the metal surfaces being joined [18].

Several studies have also identified correlating resistance spot welding parameters to tensile-shear strength for the variable response. Emre et al. [21] investigated RSW parameters using TRIP800 steel material. The method used is a two-way ANOVA analysis by using welding time and welding current for variable input. The experiment used a five-level experiment for welding time and a seven-level for welding current. The experiment's outcome was geometric nuggets and tensile-shear strength, and the result showed that the nugget diameter and the size ratio of the TRIP800 steel point weld nugget must be at least $4.5\sqrt{t}$ and 0.15–0.30. For the pull-out

failure mode, the tensile shear strength and surface quality of the nuggets are required [19].

Thakur at al. also carried out RSW research. The research used the Taguchi optimization method using a galvanized steel sheet material. The parameters used are preheating current (kA), squeeze time (cycle), current (kA), weld time (cycle), hold time (cycle), and pressure (MPa.). The optimized response parameter was the value of shear stress, which was analyzed using the ANOVA method. The analysis results showed that welding current and welding time parameters were very influential on tensile-shear strength. Meanwhile, the other two parameters, squeeze time and hold time, are less significant factors affecting the response variable [20].

Shafee et al. also conducted RSW optimization research. The study used different thicknesses of low carbon steel with a thickness of 0.8 and 1.0 mm. The research used the 3-parameter and 3-level Taguchi method. The electrode force, welding current, and welding time used for variable input. The optimized outcome (variable response) is tensile-shear strength and direct-tensile strength. The S/N ratios analysis uses higher-is-better data characteristics. ANOVA analysis result found that welding current and welding time has a significant impact on tensile-shear strength. In contrast, the direct-tensile strength parameter has significant influenced by welding time and welding current. The electrode pressure is a less significant factor in both response variables [21].

Vignesh et al. performed the RSW optimization by joining two different materials: 316L austenitic stainless steel and 2205 duplex stainless steel. The research method used the Taguchi experiment with three parameters and three levels. The optimization used some parameters such as the electrode tip (mm) diameter, welding current (kA), and the heating cycle. The experimental results were analyzed using ANOVA. The parameters that affect the

tensile-shear strength value are the welding current, heating cycle, and electrode tip diameter [16].

Unlike previous studies, this RSW study was conducted to combine two different materials: galvanized steel (SECC-AF) and low carbon steel (SPCC-SD). Both materials have slightly different properties, and due to the thickness of the zinc layer, it has a significant effect on the weldability of the SECC-AF material. The research used an experimental Taguchi by using 4-parameters, namely squeeze time (cycle), welding current (kA), welding time (cycle), and holding time (cycle). This research used a multi-level experimental, namely 2-levels for the first variable (cycle) and 3-levels for other variables. This study aims to achieve the highest tensile-shear strength and determine the effect of variations in the RSW parameters used.

2. Method

2.1. Material Selection

This study used SECC-AF and SPCC-SD plate materials with a thickness of 0.8 mm each. Galvanized steel (SECC-AF) is a kind of the Cold Rolled Coil (CRC) steel plate type, which is galvanized and annealed with the basic material of the SPCC-SD steel sheet plate. SECC-AF has the physical characteristics of a gray, slightly smooth surface like a paint primer coat. The surface coating makes the galvanized plate of SECC-AF have a higher adhesion than galvanized steel (SGCC). The SPCC-SD plate is a sheet plate that is widely used in the manufacturing industry [20]. According to the mechanical properties and chemical composition in material certificate data, the SPCC-SD (JIS 3141) steel is equivalent to the ASTM A366-91 standard [22]. The chemical composition of the selected SECC-AF and SPCC-SD steel are listed in **Table 1**. While the mechanical properties of the selected SECC-AF and SPCC-SD steel sheet are presented in **Table 2**.

Table 1. Chemical composition (in wt.%) of SECC-AF and SPCC-SD steel sheet

Element	SECC-AF		SPCC-SD	
	JIS G 3313 [23]	C9AC3360A*	JIS G 3141[24]	SP51023*
C	0.15 max.	0.0177	0.15 max.	0.0364
Mn	0.05 max.	0.0190	0.05 max.	0.0192
P	0,04 max.	0.0115	0.04 max.	0.0011
S	0.04 max.	0.0097	0.04 max.	0.0050

*The mill test certificate number

Table 2. Mechanical properties of SECC AF and SPCC-SD steel sheet

| Mechanical properties	SECC-AF		SPCC-SD	
	JIS G 3313 [23]	C9AC3360A*	JIS G 3141 [24]	SP51023*
YP (N/mm²)	240 max.	197	240 max.	195
TS (N/mm²)	370 max.	326	270 min.	315
EL (%)	30 min.	45	37 min.	45.2
Coating weight (gram /m²)	18 min	18.6	-	-
Thickness coating μm)	2.5 min	2.61	-	-

* The mill test certificate number

The coupon (specimen) is made through a shearing process. At this stage, 0.8 mm SECC-AF and SPCC-SD plate sheets cut by 25 x 105 mm, and the connection method are made to overlap the dimensions according to ASTM D1002 [25]. The tensile test samples on lap joint welded are presented in **Figure 3**.

This study used an RSW machine with a capacity of 35 kVA. The pressure on both ends of the electrodes is controlled using a pneumatic at a pressure of 3.5 MPa. The electrode type uses a tapered type electrode with a lower and upper diameter of 8 and 5 mm, respectively [10]. The compressive force at the electrode tip is calculated by the following equation:

$$F = P.A \qquad (1)$$

Where, F is the force (N), P is the pressure (N/m²), and A is the cross-sectional area (m²). With a top electrode diameter of 5 mm, the compressive force at both ends of the electrode can be calculated using equation 1, and pneumatic force of 68.7 N is obtained. **Figure 4** shows the RSW machine used in this study.
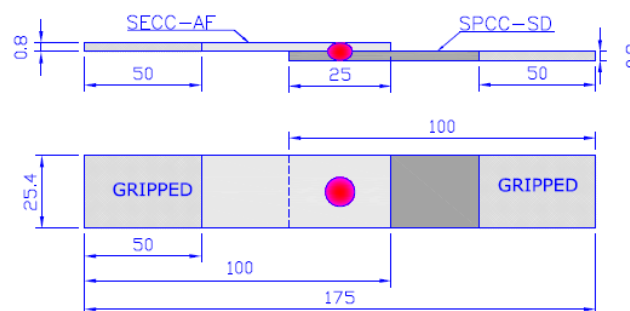
Figure 3. Tensile shear test geometry according to ASTM D1002

Figure 4. RSW machine 35 kW capacity

The RSW joining method has two failure modes, namely, pull-out mode and interface mode. The tensile failure mode is the type of failure expected as it exhibits higher joint strength than the base metal. One of the requirements to get the pull-out failure model is to meet the nugget's minimum diameter. The minimum diameter required to fulfill the failure type is specified in the Eq. (2) [5], [13].

$$D_{min} = 4.5\sqrt{t} \qquad (2)$$

Where, t is the thickness of the material, which is less than the metal is connected, this study used an SECC-AF and SPCC-SD steel sheet material 0.8 mm in the thickness. Based on the calculation with equation 3, the required of the minimum diameter nuggets is 4.27 mm. The minimum diameter is achieved by using an electrode with a diameter of 5.0 m.

Another type of failure on the RSW method is interface failure. One of the causes is the diameter of the nugget in the spot weld joint is smaller than the minimum diameter required so that the strength of the joint is weaker than the strength of the base metal [9], [10]. Another factor for interfacial mode failure is the fusion between materials during the welding process (poor welding) [11].

2.2. Process Parameters

The aim of welding parameter identification is to predict the RSW point of the welding strength. This parameter is an independent variable controlled independently, namely squeeze time (cycles), welding current (kA), welding time (seconds), and holding time (cycles). The level of each parameter is selected within limits available for welding. In the RSW process, the base metal surface conditions and the electrode temperature are difficult to control. The optimization using multi-levels experimental designs are listed in **Table 3**.
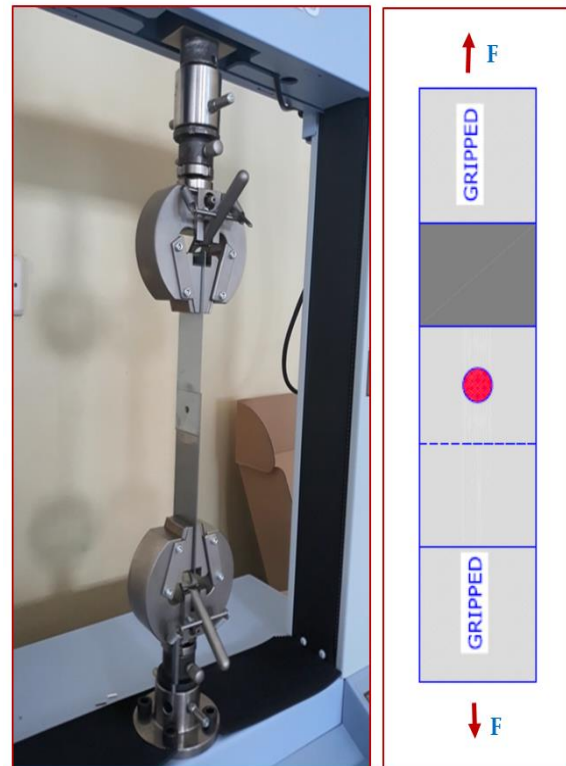
2.3. Tensile Shear Strength

The test aims to determine the ultimate tensile shear strength of the specimen. The tensile test was conducted using Shimadzu UTM model AGS-X 10kN STD E200V with 10 kN in capacity. The towing speed is controlled at 35 mm/min and the results are studied. **Figure 5** shows the testing process of the coupon.

Figure 5. Tensile shear strength test of the coupon on UTM

2.4. Orthogonal Array (OA)

One two-level and three three-level control factors were considered in this work is to obtain an optimal tensile shear strength for the RSW of dissimilar materials. The four control factors yield 9 degrees of freedom. The L18 OA has 17 degrees of freedom was selected in this work as listed in **Table 4** [26].

Table 3. RSW process parameters and their value for each level

Code	Welding parameters	LEVEL		
		I	II	III
A	Squeeze time (cycles)	20	22	-
B	Weld. current (kA)	22	25	27
C	Weld. time (seconds)	0.4	0.5	0.6
D	Hold time (cycles)	12	15	18

1 cycle=1/60 seconds

Table 4. Experimental data for tensile-shear (T-S) strength and S/N ratio

Run	A	B	C	D	Tensile shear strength (N)	SNRA
1	1	1	1	1	4453.35	72.97
2	1	1	2	2	4617.24	73.29
3	1	1	3	3	5220.09	74.35
4	1	2	1	1	5068.01	74.10
5	1	2	2	2	5126.79	74.20
6	1	2	3	3	5714.67	75.14
7	1	3	1	2	5243.61	74.39
8	1	3	2	3	5402.36	74.65
9	1	3	3	1	5629.66	75.01
10	2	1	1	3	4859.36	73.73
11	2	1	2	1	5067.84	74.10
12	2	1	3	2	5484.67	74.78
13	2	2	1	2	5611.88	74.98
14	2	2	2	3	5754.89	75.20
15	2	2	3	1	5605.31	74.97
16	2	3	1	3	5692.48	75.11
17	2	3	2	1	5821.10	75.30
18	2	3	3	2	5662.96	75.06

Multiple linear regression models are developed for tensile shear strength and nugget diameter by using statistical software. The response variable are tensile shear strength and nugget diameter whereas the predictors are A-squeeze time, B- welding current, C-welding time and D-hold time. The experimental results are used to model the response using Taguchi design [16] . The regression equation of the fitted model for tensile shear strength is obtained by tensile shear strength; N

*Tensile-shear (N) = -31461+807*A+1383*B+33708*C–173.7*D-20.64B2+1203AC-471BC +345CD*

The comparison of predicted and the experimental values of tensile shear strength for the Taguchi array is given in **Figure 6**. Predicted and experimental values of tensile shear strength. Experimental trials are conducted in random manner to validate the developed model. It is evident from the results that the developed model is capable for predicting tensile shear strength to an accuracy with the average about 0.4%.

The regression equation of the fitted model for nugget diameter is obtained by Nugget diameter; mm.

Nugget diameter (mm) = -0.850+0.1822*A+0.1227*B +0.1083*C–0.00504AB

The comparison of predicted and the experimental values of nugget diameter for the Taguchi array is given in **Figure 7**. Predicted and experimental values of nugget diameter. Experimental trials are conducted in random manner to validate the developed model. It is evident from the results that the developed model is capable for predicting nugget diameter to an accuracy with the average about 0.12%.
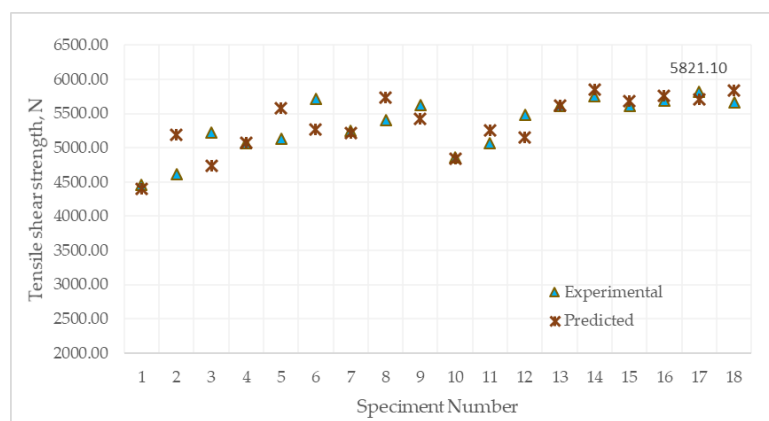
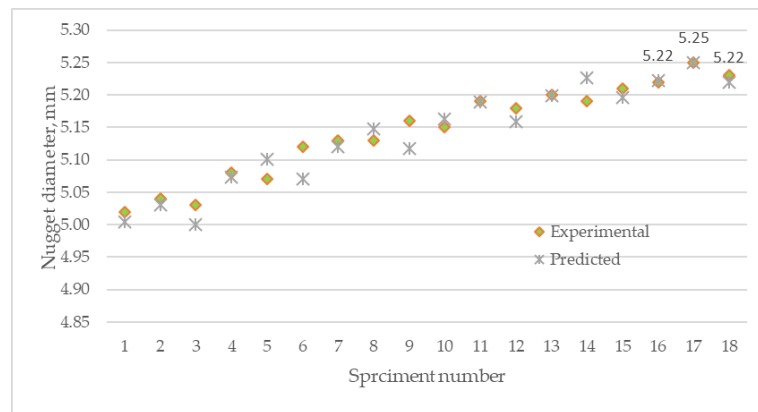**Figure 6**. Predicted and experimental values of tensile shear strength

Figure 7. Predicted and experimental values of nugget diameter

2.5. Signal to Noise Ratio (S/N Ratio)

The term S/N ratio in Taguchi's experimental technique is significant. The term 'signal' is part of the output characteristic (output /variable response). The variable response in this study is tensile-shear strength. In contrast, the term 'noise' represents an undesirable value for the output characteristic. The S/N ratio shows the best parameter, which will give the best or optimal output characteristic value [27]. The S/N ratio calculation is carried out depending on the characteristics of the desired data quality. The Taguchi method gives the output data quality characteristics into three parts: smaller is better, larger is better, and nominal is the best. The mathematical equations for each output characteristic are shown in equations 3, 4 and 5 [28].

Smaller is better:

$$S/N \ ratio \ = -10 \log \sum_{i=1}^{n_0} \frac{y_i^2}{n_0} \qquad (3)$$

Larger is better:

$$S/N \ ratio \ = -10 \log \frac{1}{n_0} \sum_{i=1}^{n_0} \frac{1}{y_i^2} \qquad (4)$$

Nominal is the best:

$$S/N \ ratio \ = -10 \log \frac{\bar{y}^2}{s^2} \qquad (5)$$

Where n_0 is the number of samples, y_i is the response factor, $\bar{y}$ is the mean of the responding factor, and s is the variant of the response factor.

3. Result and Discussion

3.1. Tensile Shear Strength Analysis

Two sample is welded in each iteration or series for static tensile shear strength and evaluation nugget diameter. All samples tested for tensile shear strength successfully experienced a pull-out failure mode. It is meant that the fusion during the RSW joining process between SECC-AF and SPCC-SD metals for all parameters is performing well. All the parameters tested have worked in melting the 2.5-micron zinc layer on the SECC-AF steel material. The pull-out failure mode on the steel coupling SECC-AF and SPCC-SD is shown in **Figure 8**.

Figure 8. Pull-out failure mode for iteration 16, 17 and 18

Figure 8 shows the achievable of the best fusion in the nugget area of the joining material of SECC-AF and SPCC-SD. The seventeenth iteration in table 4 showed the highest tensile shear strength with a value of 5821.10 N with RSW parameters of 22 cycles of squeeze time, 27 kA of welding current, and 0.5 seconds welding time, and 12 cycles of holding time. The tensile shear strength test graph is presented in **Figure 9**.

3.2. S/N Ratio Analysis.

To measure each parameter level's effect, an S/N ratio analysis has been carried out. The mean S/N ratio at levels 1, 2, and 3 were calculated using
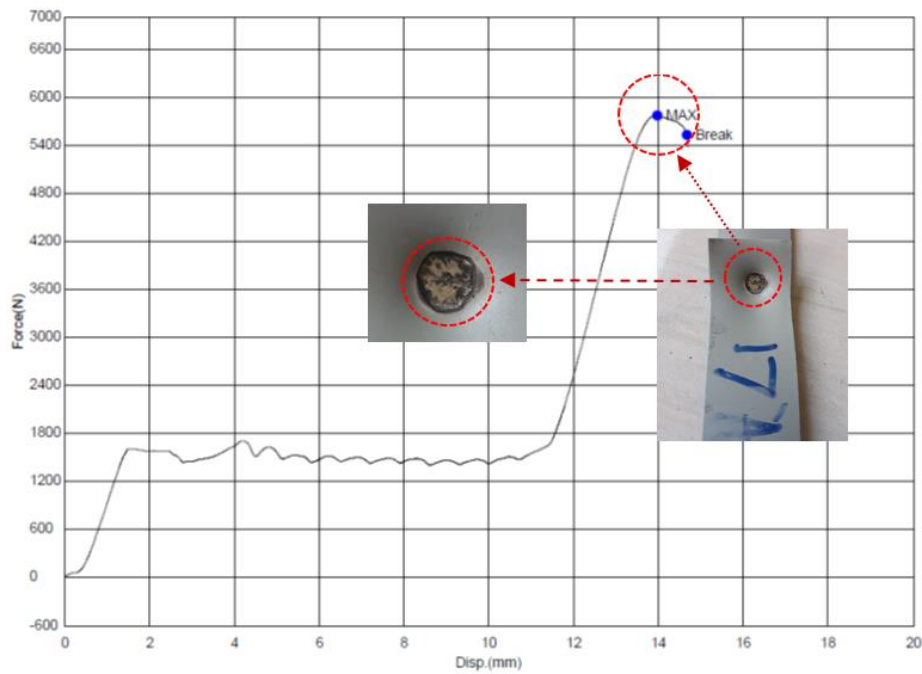
Figure 9. The highest tensile shear strength (force) result

Eq. (4). Parameters with large differences mean a high effect on the response. In this research, the tensile shear strength of the nuggets makes the welding current the most considerable difference according to the levels. In contrast, each level of the squeeze time parameter shows a smaller effect on the output. Based on the S/N ratio in figure 10, the new welding operation parameters are obtained through each parameter's maximum level. To get optimum tensile shear strength (T-S), an S/N ratio plot suggesting parameter settings such as squeeze time level 2, welding current level 3, welding time level 3, and hold time level 3. **Figure 10** shows the S/N ratio plot referred to in the points mentioned above. To get the optimum average tensile shear strength, **Figure 11** also suggests the same parameter settings as in the previous graph, namely squeeze time at level 2, welding current at level 3, welding time at level 3, and hold time at level 3.
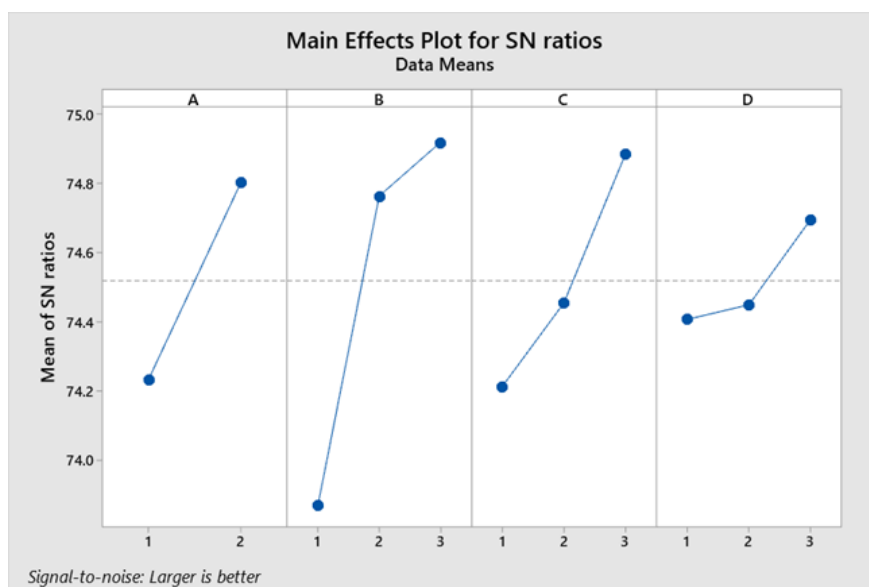

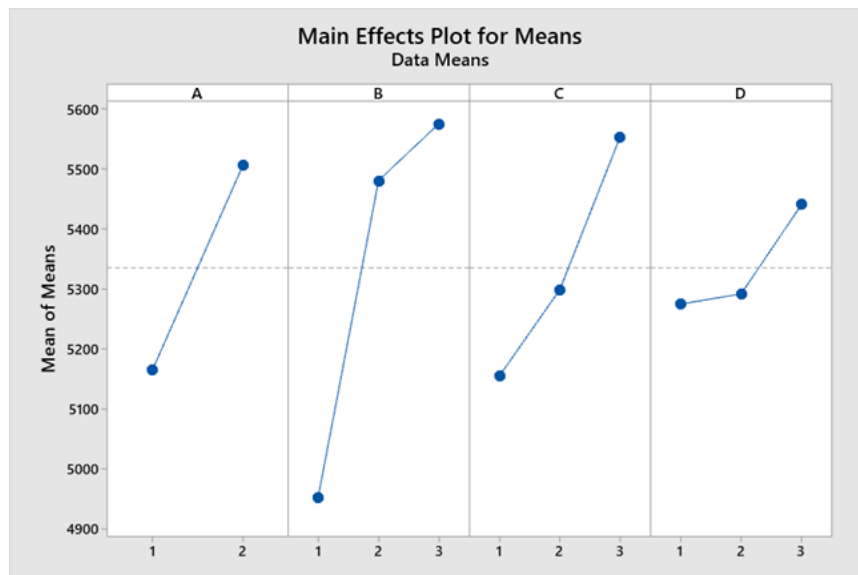**Figure 10**. S/N ratio output for tensile shear strength

Figure 11. S/N ratio output for tensile shear strength

The input parameter that most influences the variable response (T-S Strength) in the incorporation of SEECC-AF and SPCC materials is the welding current with a delta value of 1.05. Other significant parameters are influenced by followed welding time, squeeze time , and holding time, with delta values of 0.67, 0.57, and 0.29, respectively. The response table for the S/N ratio for each parameter of resistance spot welding is presented in **Table 5**.

Table 5. Response table for larger S/N Ratios is better

Level	Squeeze time	Weld. current	Weld. time	Hold time
1	74.23	73.87	74.21	74.41
2	74.80	74.76	74.46	74.45
3		74.92	74.89	74.70
Delta	0.57	1.05	0.67	0.29
Rank	3	1	2	4

This study confirmed previous research conducted by Takur et al [20], that welding current and welding time are significant parameters affecting tensile shear strength.

4. Conclusion

Setting the correct parameters in the RSW process involving using a pneumatic force on the tip of the electrode, which is set at 68.7 N, especially spot welding to join the galvanized steel to low carbon steel materials, has proven successful. Two critical parameters that are used to obtain the highest tensile shear strength are welding time and welding current. The parameter in the seventeenth iteration achieved the highest tensile shear strength and nugget diameter. These have achieved on 22 squeeze time cycles, 27 kA of welding current, and 0.5 seconds of welding time, and 12 holding time cycles. The parameters of welding time and welding current also have a significant influence in preventing the occurrence of interfacial failure mode. The next research will be conducted for looking for the zinc layer thickness's effect on the tensile shear strength and diameter of the nuggets.

_____

Author's Declaration

Authors' contributions and responsibilities

The authors made substantial contributions to the conception and design of the study. The authors took responsibility for data analysis, interpretation and discussion of results. The authors read and approved the final manuscript.

Availability of data and materials

All data are available from the authors.

Competing interests

The authors declare no competing interest.

Additional information

No additional information from the authors.

_____

References

[1] BSN, *Galvanisasi (hot dip galvanized) pada besi dan baja fabrikasi - Spesifikasi dan metode pengujian*. Indonesia, 2004.

[2] K. Wibisono, "Pabrik baja galvanis KNSS pertama di Indonesia selesai 60 persen," *AntaraNews*, Jakarta, Mar-2016.

[3] R. Mazumdar, "Government may force automakers to use 70 per cent galvanised steel in car body," *The Economic Times*, Aug-2018.

[4] M. P. Mubiayi, E. T. Akinlabi, and M. E. Makhatha, *Current Trends in Friction Stir Welding (FSW) and Friction Stir Spot Welding (FSSW)*, vol. 6. 2019.

[5] J. Pan and K. Sripichai, "Mechanics modeling of spot welds under general loading conditions and applications to fatigue life predictions," *Woodhead Publishing Limited*, 2010.

[6] A. H. Ertas and F. O. Sonmez, "Design optimization of spot-welded plates for maximum fatigue life," *Finite Elements in Analysis and Design*, vol. 47, no. 4, pp. 413–423, 2011.

[7] D. Ren, D. Zhao, L. Liu, and K. Zhao, "Clinch-resistance spot welding of galvanized mild steel to 5083 Al alloy," *The International Journal of Advanced Manufacturing Technology*, vol. 101, no. 1–4, pp. 511–521, 2019.

[8] Y. G. Kim, D. C. Kim, and S. M. Joo, "Evaluation of tensile shear strength for dissimilar spot welds of Al-Si-Mg aluminum alloy and galvanized steel by delta-spot welding process," *Journal of Mechanical Science and Technology*, vol. 33, no. 11, pp. 5399–5405, 2019.

[9] S. H. M. Anijdan, M. Sabzi, M. Ghobeiti-hasab, and A. Roshan-ghiyas, "Optimization of spot welding process parameters in dissimilar joint of dual phase steel DP600 and AISI 304 stainless steel to achieve the highest level of shear-tensile strength," *Materials Science & Engineering A*, vol. 726, no. April, pp. 120–125, 2018.

[10] D. L. Olson, S. Thomas A., S. Liu, Edwards, and R. A Glen, *ASM Vol 6 Welding, Brazing, And Soldering*, vol. 165. 2019.

[11] Miller Handbook, *Handbook for Resistance Spot Welding*. Miller Electric Mfg. Co., 2010.

[12] E. Gunawan, Sukarman, A. D. Shieddieque, C. Anwar, and Jatira, "Optimasi Parameter Proses Resistance Spot Welding pada Pengabungan Material SECC-AF," in *Seminar Nasional Teknologi dan Riset Terapan*, 2019, no. September, pp. 132–137.

[13] P. S. Wei and T. H. Wu, "Electrode geometry effects on microstructure determined by heat transfer and solidification rate during resistance spot welding," *International Journal of Heat and Mass Transfer*, vol. 79, pp. 408–416, 2014.

[14] H. Wiryosumarto and T. Okumura, *Teknologi Pengelasan Logam*, 8th ed. Jakarta: PT Pradnya Paramita, 2000.

[15] J. P. Oliveira, K. Ponder, E. Brizes, T. Abke, A. J. Ramirez, and P. Edwards, "Combining resistance spot welding and friction element welding for dissimilar joining of aluminum to high strength steels," *Journal of Materials Processing Technology*, vol. 273, no. January, p. 116192, 2019.

[16] K. Vignesh, A. E. Perumal, and P. Velmurugan, "Optimization of resistance spot welding process parameters and microstructural examination for dissimilar welding of AISI 316L austenitic stainless steel and 2205 duplex stainless steel," *The International Journal of Advanced Manufacturing Technology*, vol. 93, pp. 455–465, 2017.

[17] M. Tumuluru, *Resistance spot weld performance and weld failure modes for dual phase and TRIP steels*. Woodhead Publishing Limited, 2010.

[18] P. Muthu, "Optimization of the Process Parameters of Resistance Spot Welding of

AISI 316l Sheets Using Taguchi Method," *Mechanics and Mechanical Engineering*, vol. 23, no. 1, pp. 64–69, 2019.

[19] H. E. Emre and R. Kaçar, "Development of weld lobe for resistance spot-welded TRIP800 steel and evaluation of fracture mode of its weldment," *International Journal of Advanced Manufacturing Technology, Springer*, vol. 85, pp. 1737–1747, 2016.

[20] A. G. Thakur and V. M. Nandedkar, "Optimization of the Resistance Spot Welding Process of Galvanized Steel Sheet Using the Taguchi Method," Arabian Journal for Science and Engineering, vol.39, pp. 1171–1176, 2014.

[21] S. Shafee, B. B. Naik, and K. Sammaiah, "Resistance Spot Weld Quality Characteristics Improvement By Taguchi Method," *Materials Today: Proceedings*, vol. 2, no. 4–5, pp. 2595–2604, 2015.

[22] W. Stichel, *Handbook of comparitative world steel standards; USA-United Kingdom-Germany-France-Russia-Japan-Canada-Australia-International. Hrsg.: Albert & Melilli, 552 Seiten. ASTM Data Series DS 67, American Society for Testing and Materials, PA, USA 1996, £ 195.00*, vol. 48, no. 6. 1997.

[23] Japanese Standards Association, *JIS G 3313 Electrolytic zinc-coated steel sheet and coils*. 1998, pp. 428–480.

[24] Japanese Standards Association, *JIS G 3141 Cold-reduced carbon steel sheets and strip*. 2005.

[25] ASTM International, *ASTM D1002 Standard Test Method for Apparent Shear Strength of Single-Lap-Joint Adhesively Bonded Metal Specimens by Tension Loading (Metal-to-Metal)*. 2019.

[26] P. J. Ross, *Taguchi Techniques for Quality Engineering*. New York: Tata McGraw-Hill, 2005.

[27] A. Abdulah, S. Sukarman, C. Anwar, A. Djafar Shieddieque, and A. Ilmar Ramadhan, "Optimization of yarn texturing process DTY-150D/96F using taguchi method," *Technology Report of Kansai University*, vol. 62, no. 4, pp. 1471–1479, 2020.

[28] S. F. Arnold, *Design of Experiments with MINITAB*, vol. 60, no. 2. 2006.